Exploring Key Processes in Modeling the Madden-Julian Oscillation (MJO):
The WCRP-WWRP YOTC MJO Task Force / GEWEX GASS MJO Global Model Evaluation Project

Xianan Jiang[1,2], Nicholas Klingaman[4], Prince Xiavier[3] , Duane E. Waliser[2] , Jon Petch[3], Steve Woolnough[3]

[1]Joint Institute for Regional Earth System Sci. & Engineering, University of California, Los Angeles, CA; [2]Jet Propulsion Laboratory, Pasadena, CA; [3]UK Met Office; [4]University of Reading, UK ; **Project website:** http://www.ucar.edu/yotc/mjodiab.html; **Contact Email:** xianan@ucla.edu

Introduction

While the Madden-Julian Oscillation (MJO) exerts pronounced influences on global climate and weather systems, and represents the primary source of predictability on subseasonal time scales, our general circulation models (GCMs) exhibit rather limited capability in representing this prominent tropical variability mode. Meanwhile, the fundamental physics of the MJO are still elusive.

A joint project (Petch et al. 2011) for global model intercomparison of the physical processes associated with the MJO was launched by the GEWEX Global Atmospheric System Studies (GASS) and the WCRP-WWRP/THORPEX Year of Tropical Convection (YOTC; Waliser et al. 2011) MJO Task Force (MJOTF). The goal of the project was to provide a framework for model developers to make improvements to the physical schemes in global weather and climate models. One important component of the comparison will characterize, compare and evaluate the heating, moistening and momentum mixing processes associated with the MJO by examining vertical profiles of model physical tendencies collected from this project.

Experimental Components of the MJOTF/GASS MJO Project

Model Experiment	Science Focus	Exp. POC
I. 20 Yr Climatological Simulations (1991-2010 if AGCM) 6-hr, Global Output Vertical Structure, Physical Tendencies	Model MJO Fidelity Vertical structure Multi-scale Interactions: (e.g., TCs, Monsoon, ENSO)	UCLA/JPL X. Jiang D. Waliser
II. 2-Day MJO Hindcasts YOTC MJO Cases E & F (winter 2009)* Time Step, Indo-Pacific Domain Output Very Detailed Physical/Model Processes	Heat and moisture budgets Model Physics Evaluation (e.g. Convection/Cloud/BL) Short range Degradation	Met Office P. Xavier J. Petch
III. 20-Day MJO Hindcasts YOTC MJO Cases E & F (winter 2009)* 3-hr, Global Output Elements of I & II	MJO Forecast Skill State Evolution/Degradation Elements of I & II	U. Reading N. Klingaman S. Woolnough

*DYNAMO Case TBD

Model output characteristics, science focus and POCs for the three model components.

The experiment takes advantage of the links between model biases in short-range forecasts and long-term climate simulations, and evaluates these in the context of the MJO. Three types of simulations were carried out during this project:

I. 20-year climate simulations that provide a characterization of the models' intrinsic capabilities of representing MJO variability.

II. A series of daily initialized hindcasts for a lead-time of 2 days with time-step output for two MJO events within the YOTC period—specifically the two successive MJO events (Case E & F; see right) during boreal winter 2009-2010.

III. Similarly as in II), but for daily hindcasts with lead time from 1 to 20 days, to explore model skill in predicting the MJO.

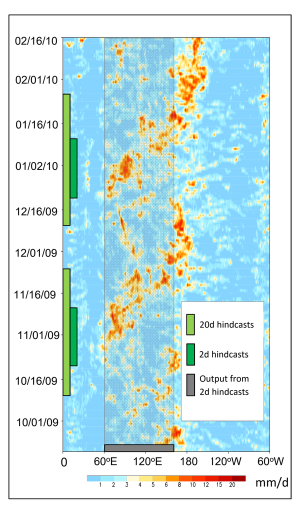

Participating Models

No	Model	Point of Contact	Institution	Experiment: Climate Simulation	Short-term Hindcast	Long-term Hindcast
01	01_GEOS-5 AGCM	Siegfried Schubert; Hailan Wang	NASA/GMAO	X	X	X
02	03a_SPCCSM 03b_SPCAM	David Randall; Charlotte Demott; Cristiana Stan	CSU, COLA	X		
03	03c_SPCAM	Mike Pritchard (UW)	UCSD		X	X
04	04_GISS_ModelE2	Daehyun Kim; Anthony Del Genio	LDEO	X		X
05	05_EC_GEM	Hai Lin	Environment Canada	X		X
06	06_NICAM	Masaki Satoh ; Tomoe Nasuno	AORI, U. Tokyo /JAMSTEC			X
07	07_MIROC5.0	Tomoki Miyakawa	AORI/Univ. Tokyo	X	X	X
08	10_MRI-GCM	Eiki SHINDO; Akio Kitoh	MRI	X	X	X
09	11_CWB AGCM	Mong-Ming Lu; Hsin-Hsing Chia; Hsiao-Chung Tsai	CWB, Taiwan	X		
10	12_PNNL_WRF	Samson M Hagos	PNNL		X	
11	14_PNU_CFS	Kyong-Hwan Seo	PNU	X		
12	15_ECMWF_IFS	Frederic Vitart	ECMWF	X	X	X
13	16_MPI_ECHAM6	Traute Crueger	ZMAW	X	-	-
14	17_MetUM GA3.0	Prince Xavier	Met Office UK	X	X	X
15	21_NCAR_CAM5	Rich Neale; Cecile Hannay	NCAR	X	X	X
16	22_NAVGEM	Jim Ridout; Maria Flatau	NRL	X	X	X
17	24_CAM5/CAMS	Guang Zhang; Aneesh Subramanian	UCSD	X	-	-
18	27_CFSv2	Wanqiu Wang	NCEP/CPC	X	-	X
19	30_GFSv2	Arindam Chakraborty	Indian Inst of Sci.	-	-	X
20	31a_CNRM_AM 31b_CNRM_CM 31c_CNRM_ACM	Gilles Bellon; Romain Roehrig	CNRM/France	X	-	X
21	34_CanCM4	John Scinocca; Bill Merryfield	CCCma	X	X	X
22	35_BCCAGCM2.1	Tongwen Wu, Jie Zhang	Nat. Climate Center, China	X	X	
23	36_FGOALS2.0-s	Wenting Hu	LASG/IAP, China	X	-	-
24	37_ECHAM5-SIT	Wan-Ling Tseng; Noel Keenlyside	Univ of Bergen	X	-	-
25	39_Modified CAM4	Courtney Schumacher; Cara-Lyn Lappen	Texas A & M U.	X		
26	40_ACCESS	Hongyan Zhu	BoM, Australia	X	X	X
27	43_ISUGCM	Xiaoqing Wu	Iowa State University	X	-	-
28	44_CAM5ZMMicro	Hsi-Yen Ma	LLNL	X	X	X
29	45_ECEARTH3	Klaus Wyser; Mihaela Caian	SMHI	X	X	X

Amplitude of the Intra-seasonal Variability in Climate Models

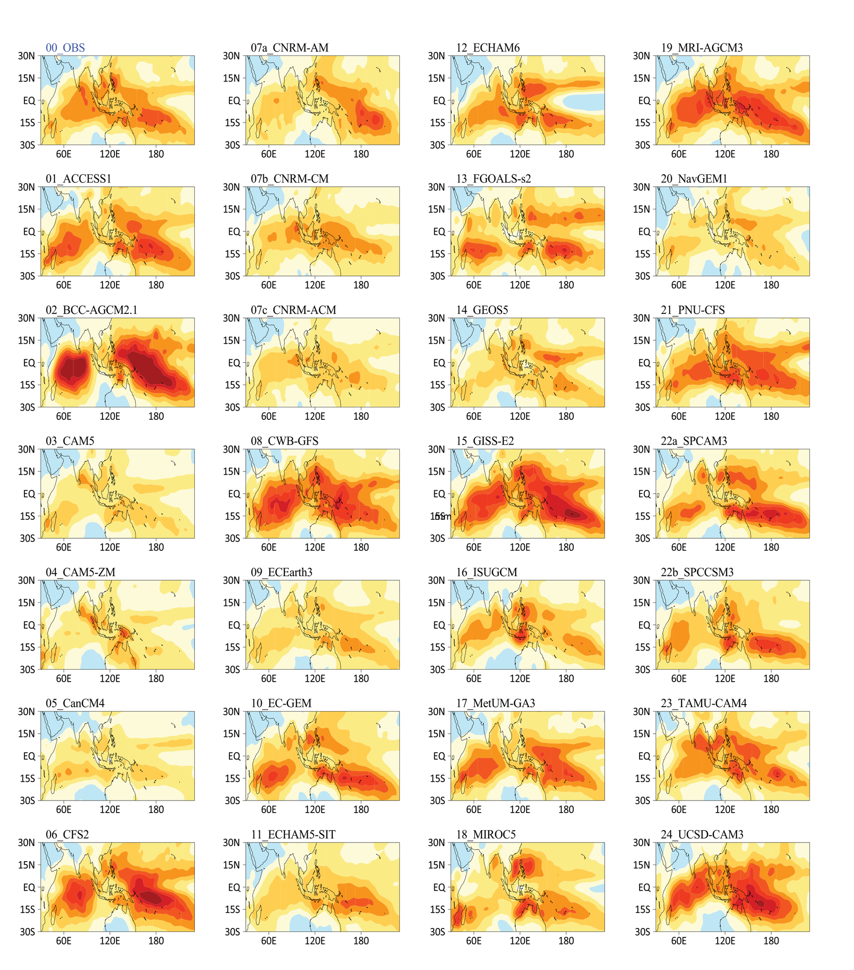

Standard deviation of daily 20-100-day bandpass filtered rainfall anomalies during boreal winter (Nov-Apr) based on observations and model simulations (unit: mm day^{-1}).

Model Fidelity in Representing the MJO Propagation

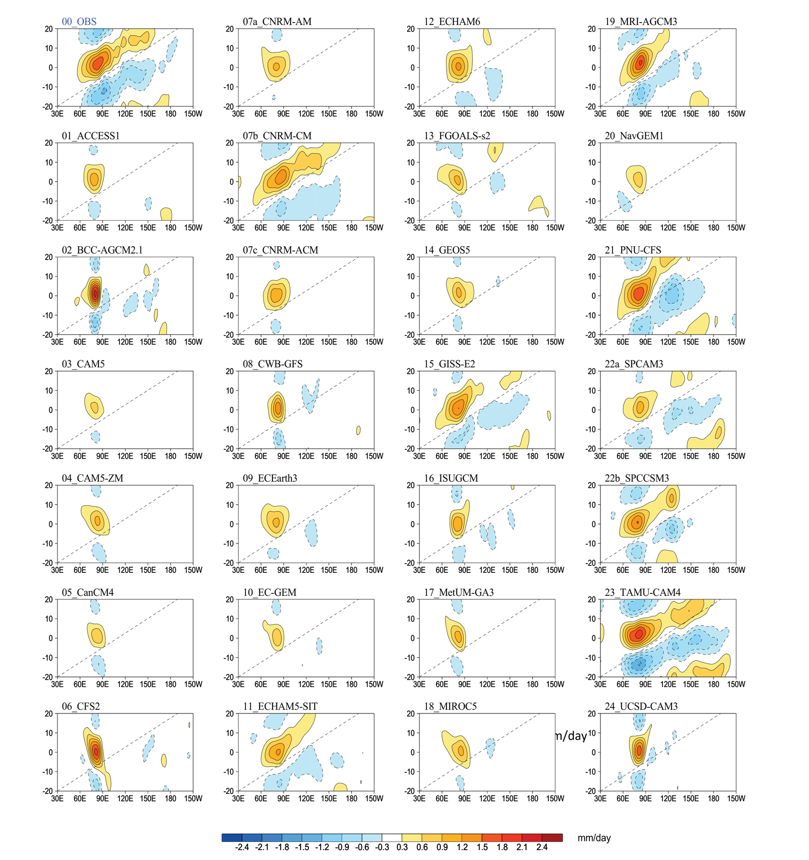

Longitude-time evolution of rainfall anomalies by lag-regression of 20-100-day bandpass filtered anomalous rainfall against itself averaged over the equatorial Eastern Indian Ocean (75–85°E; 5°S–5°N). Rainfall anomalies are averaged over 10°S–10°N. Dashed lines in each panel denote the 5 ms^{-1} eastward propagation phase speed.

MJO Skill by Patt. Correlations of Hovmoller Diagrams

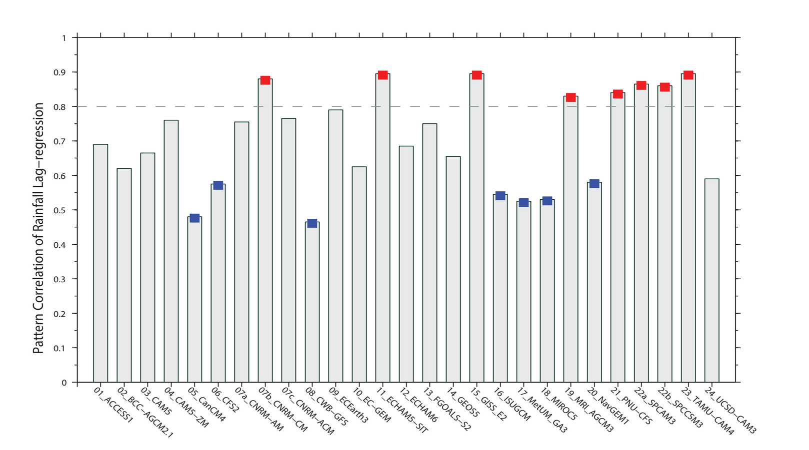

MJO skill scores in GCMs based on pattern correlations of lag-regressed rainfall anomalies on a time-longitude domain (60ºE-180; day -20 to day 20) to the observations. Red and blue squares denote GCMs simulating strong and weak eastward propagation of the MJO.

Wavenumber-frequency Spectra of Rainfall in GCMs

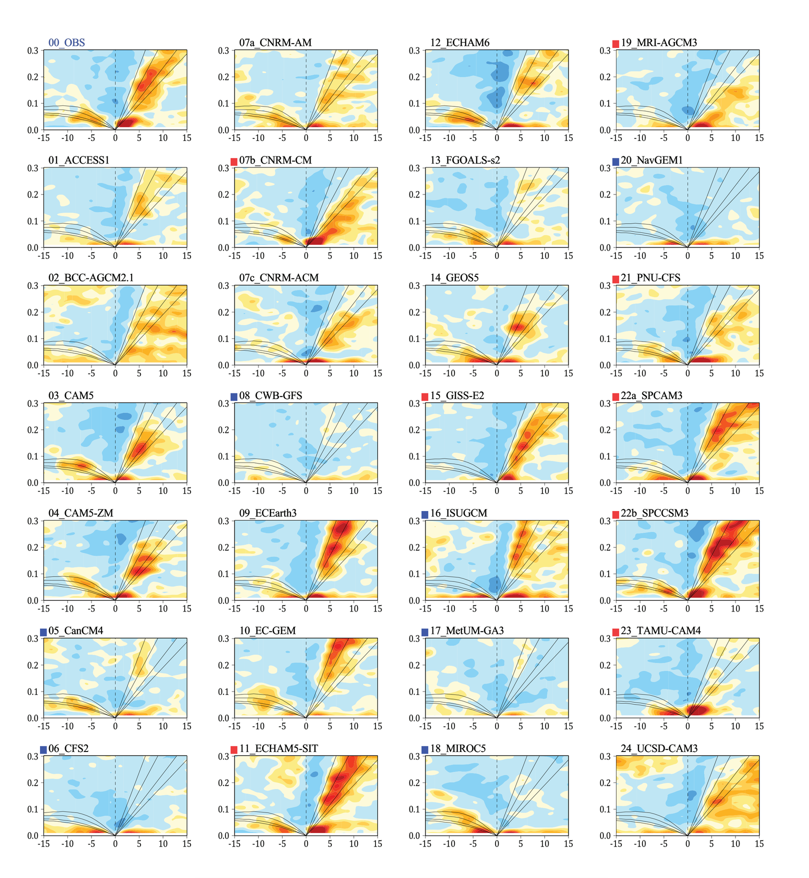

Wavenumber-frequency power spectra of the symmetric component of equatorial rainfall over the eastern hemisphere (60ºE-180º), plotted as the ratio between raw rainfall power and the power in a smoothed red-noise background spectrum averaged from 15ºS to 15ºN. Superimposed are the dispersion curves of the equatorial waves for the four equivalent depths of 9, 12, 25, and 50m. Red and blue squares denote good and poor MJO GCMs.

Vertical Structure of MJO in "Good" and "Bad" GCMs

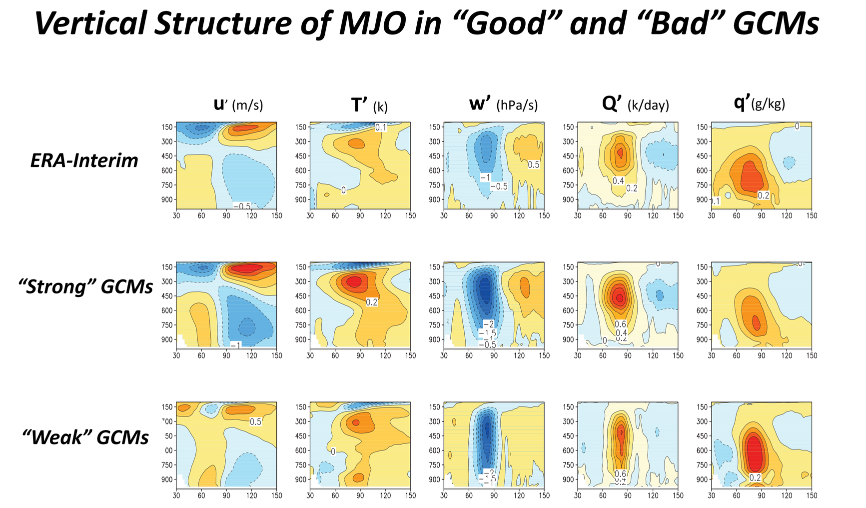

Vertical–longitudinal profiles of zero-lag regressed zonal wind (u), temperature (T), vertical velocity (w), diabatic heating (Q), and specific humidity (q) onto 20–90-day bandpass-filtered Indian Ocean rainfall (75-85°E; 5°S-5°N) based on ERA-Interim (top), composites over good (middle) and poor (bottom) MJO GCMs. All variables are averaged over 10°S–10°N. For model composite results, only those significant at 95% level are shown by shaded color.

Process-oriented Diagnosis for MJO skill in GCMs

Convective Sensitivity to Environment Moisture

(Kim et al. 2014; Maloney et al. 2014)

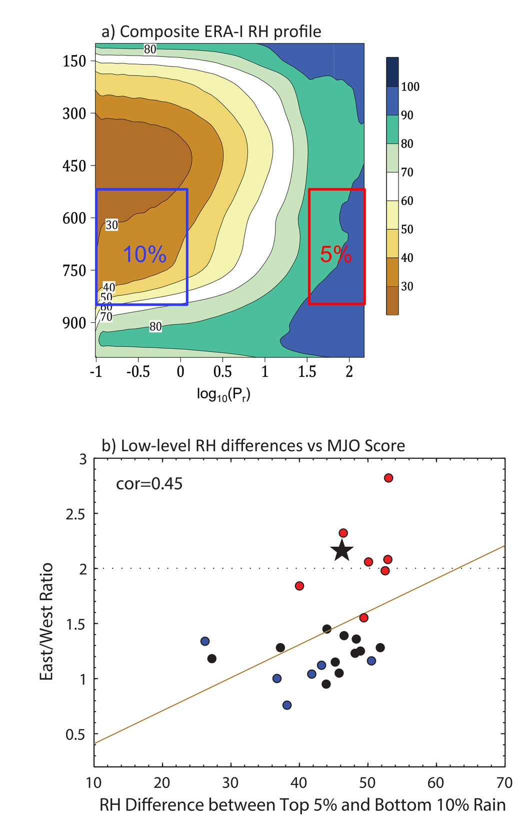

(a) Composite vertical structure of relative humidity based on ERA-Interim as a function of TRMM rain rate over the Indo-Pacific domain (60˚E-180˚; 15˚S-15˚N) for November-April during the period of 1998-2012. Note that the rain rate on x-axis is plotted on a log10 scale; (b) MJO skill score (E/W ratio) versus 500-850hPa mass weighted relative humidity difference between the top 5% and bottom 10% of daily rainfall events in observations (star mark) and GCM simulations (dots; red and blue for good and poor MJO GCMs, respectively).

Normalized Gross Moist Stability (NGMS)

(Raymond et al. 2008; Benedict et al. 2013; Maloney et al. 2014)

$$\Gamma_T = -\frac{T_R\langle V\nabla s+\omega\partial s/\partial p\rangle}{L\langle\nabla\cdot(rV)\rangle}$$ *s:* moist entropy; *r:* mixing ratio

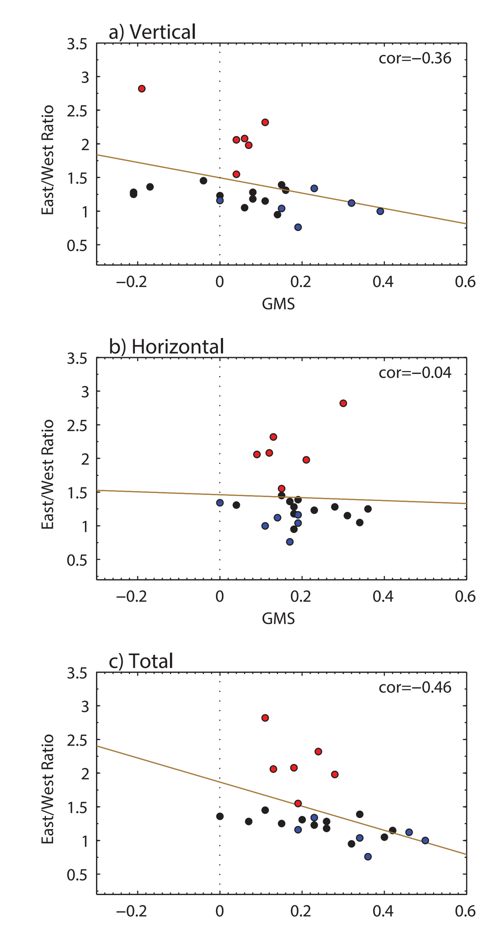

MJO skill score (E/W ratio) versus the (a) vertical component, (b) horizontal component, and (c) total gross moist stability averaged on oceanic grid points over the domain of 60˚-150˚E and 15˚S-15˚N. Red and blue dots represent GCMs with good and poor MJO. The correlation and least-square regression line are also shown in each panel.

Radiative and surface fluxes vs MJO Amplitude

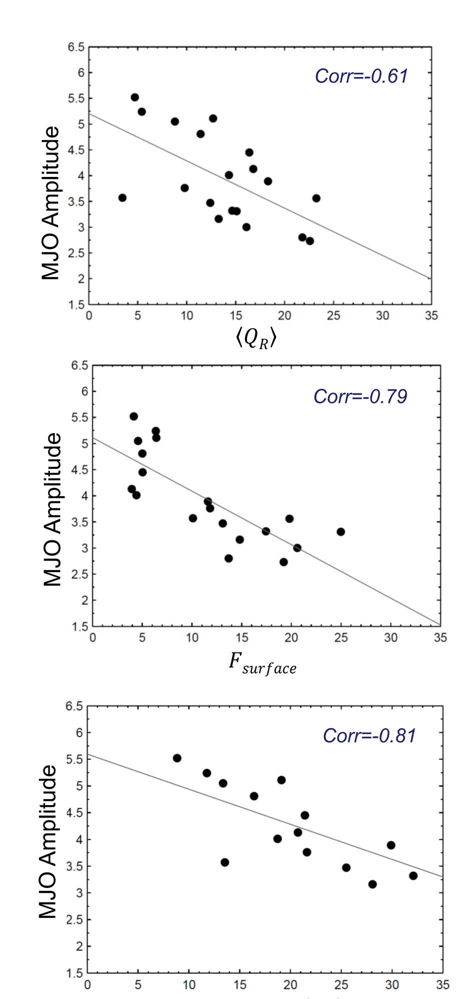

MJO amplitude (mm day^{-1}), as denoted by standard deviation of 20-100-day filtered rainfall over the Indo-Pacific warm pool during boreal winter, versus total anomalous energy sources by vertically integrated radiative heating (a), surface fluxes (b), and total flux (c), averaged over the MJO convection center in the Indian Ocean (75-85ºE; 10ºS-10ºN; unit: w m^{-2}) corresponding to 3 mm day^{-1} rainfall anomalies across model simulations. Both anomalous radiative heating and surface fluxes associated with the MJO were derived by lag-0 regression onto 20-100-day band-pass filtered rainfall over the Indian Ocean box (75-85ºE; 5ºS-5ºN).

MJO skill in climate simulations and hindcasts

MJO predictive skill in 20-day hindcasts

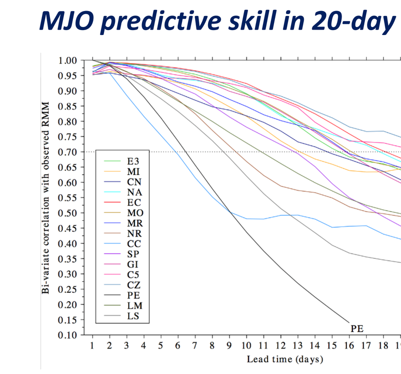

Bivariate correlations with lead time of hindcast and observed two Real-time Multivariate MJO (RMM) indices. Black lines ("PE") is from persistence forecasts.

MJO fidelity in 20-day hindcasts vs skill in climate simulations

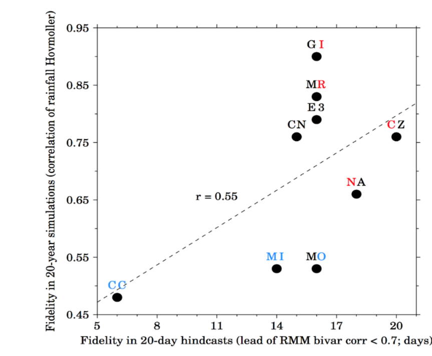

MJO fidelity in climate simulations is based on pattern correlations of rainfall Hovmoller diagrams between each GCM and observations, while for 20-day hindcasts, it is measured by the first lead time at which the bivariate correlations of the simulated and observed RMM indices below 0.7.

Moistening Processes and MJO Fidelity

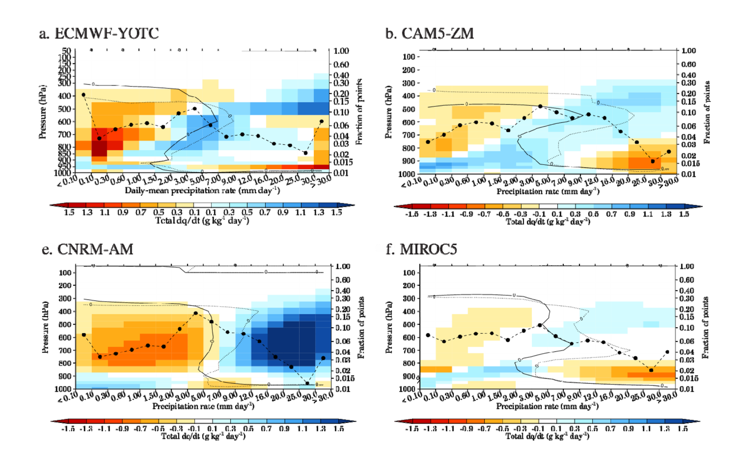

(Shading) Mean vertical profiles of the rate of change of specific humidity (dq/dt; g kg d^{-1}) for each range of rain rates on the horizontal axis. Solid (dotted) lines are zero contours of the dq/dt from GCM dynamics (physics). Dynamics tendencies are positive (moistening) above and to the right of the solid line; physics tendencies are positive below and to the left of the dotted line. Dashed lines show probability distribution functions (PDFs) of rain rates, using the right-hand vertical axis. Composites are computed from 3h data for 20-day hindcasts.

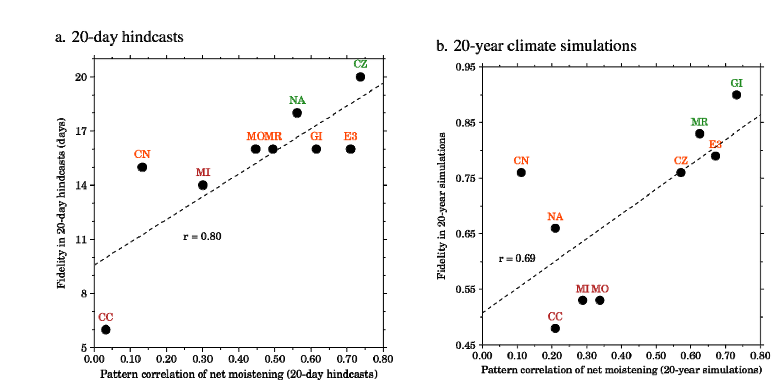

Model skill in the net moistening diagnostics as derived by pattern correlations of net moistening against ECMWF-YOTC versus MJO fidelity in 20-day hindcasts (left) and 20-year climate simulations (right).

Summary

- The Madden-Julian Oscillation (MJO) remains a great challenge in our latest generation GCMs. The systematic eastward propagation of the MJO is only well simulated in about one fourth of the total participating models in the recent MJOTask Force / GEWEX GASS MJO Project.
- Two metrics, including the low-level relative humidity difference between high- and low-rain events and seasonal mean gross moist stability, exhibit statistically significant correlations with the MJO performance in climate simulations.
- Increased cloud-radiative and wind evaporation feedbacks tend to be associated with reduced amplitude of intraseasonal variability, which is incompatible with the radiative instability theory previously proposed for the MJO.
- Models that performed well in hindcast mode (for these two cases) do not necessarily perform well in climate mode, and vice versa.
- A modest relationship is found between MJO fidelity and net moistening based on 20-day hindcast and climate simulations, with the highest-fidelity models showing low- and mid-level moistening at light to moderate rain rates.

Publications & Data Archive

Petch, et al., 2011. A Global Model Intercomparison of the Physical Processes Associated with the Madden-Julian Oscillation, WCRP GEWEX News, Vol. 21, No. 3, pages 3-5.

Jiang, et al, 2015: Vertical structure and diabatic processes of the Madden-Julian Oscillation: Exploring Key Model Physics in Climate Simulations, Journal of Geophysical Research - Atmosphere, 120, DOI:10.1002/2014JD022375, 4718-4748.

Xavier, et al., 2015: Vertical structure and diabatic processes of the Madden-Julian Oscillation: Biases and uncertainties at short range, Journal of Geophysical Research - Atmosphere, 120, DOI: 10.1002/2014JD022718, 4749–4763.

Klingaman, et al, 2015a: Vertical structure and diabatic processes of the Madden-Julian Oscillation: Linking hindcast fidelity to simulated diabatic heating and moistening, Journal of Geophysical Research - Atmosphere, 120, DOI: 10.1002/2014JD022718, 4749–4763.

Klingaman, et al., 2015b: Vertical structure and diabatic processes of the Madden-Julian Oscillation: Synthesis and summary, Journal of Geophysical Research - Atmosphere, 120, DOI: 10.1002/2015JD023196, 4671-4689.

Model output can be obtained from ESGF: https://earthsystemcog.org/projects/gass-yotc-mip/

This project has been supported by US NSF Climate and Large-Scale Dynamics Program, NOAA Climate Program Office MAPP and CVP Programs, and NAVY ONR.